Published online 16 May 2011 *Nucleic Acids Research, 2011, Vol. 39, No. 15* ***6729–6740***
doi:10.1093/nar/gkr206

An RNA aptamer perturbs heat shock transcription factor activity in *Drosophila melanogaster*

H. Hans Salamanca[1], Nicholas Fuda[1], Hua Shi[2] and John T. Lis[1,3,*]

[1]Department of Molecular Biology and Genetics, Cornell University, Ithaca, NY 14853, [2]Department of Biological Sciences and Institute for RNA Science and Technology, University at Albany, State University of New York, Albany, NY 12222, USA and [3]Department of Biomedical Engineering, Dongguk University, Seoul, South Korea

Received December 7, 2010; Revised March 19, 2011; Accepted March 21, 2011

ABSTRACT

Heat shock transcription factor (HSF1) is a conserved master regulator that orchestrates the protection of normal cells from stress. However, HSF1 also protects abnormal cells and is required for carcinogenesis. Here, we generate an highly specific RNA aptamer (iaRNA^{HSF1}) that binds *Drosophila* HSF1 and inhibits HSF1 binding to DNA. In *Drosophila* animals, iaRNA^{HSF1} reduces normal *Hsp83* levels and promotes developmental abnormalities, mimicking the spectrum of phenotypes that occur when Hsp83 activity is reduced. The HSF1 aptamer also effectively suppresses the abnormal growth phenotypes induced by constitutively active forms of the EGF receptor and Raf oncoproteins. Our results indicate that HSF1 contributes toward the morphological development of animal traits by controlling the expression of molecular chaperones under normal growth conditions. Additionally, our study demonstrates the utility of the RNA aptamer technology as a promising chemical genetic approach to investigate biological mechanisms, including cancer and for identifying effective drug targets *in vivo*.

INTRODUCTION

HSF1 is a highly conserved transcription factor that responds to a variety of signals to regulate the expression of a broad spectrum of target genes (1,2). HSF1 activity in *Drosophila* and *Saccharomyces cerevisiae* is encoded by a single *HSF1* gene; while in mammals and plants multiple isoforms exist that appear to have specialized functions (3–6). In response to thermal exposure, HSF1 is responsible for activating the heat shock (HS) response, a highly conserved mechanism among different kingdoms (7). During this response, HSF1 activates the expression of a specific set of HS genes, resulting in the accumulation of proteins possessing chaperoning activities that allow organisms to cope with cellular damage induced by thermal stress. Additionally, HSF1 activity has been shown to be important during certain cell and developmental processes in various organisms. In *S. cerevisiae*, HSF1 is essential for cell viability and for vegetative growth (8). Unlike yeast, animals do not require HSF1 activity for general cell growth; rather HSF1 is required during specific developmental stages. For instance, in *Drosophila*, HSF1 activity is required for early larval development and during oogenesis (9); while in *Caenorhabditis elegans*, HSF1 has been shown to be required for maintenance of longevity (10,11). Mammals have evolved multiple HSFs with specialized functions which appear to play multiple regulatory roles during development that extend beyond the HS/stress response (2–5).

Although mouse HSF1 activity is not required for animal viability, it does protect cells from cellular insults (4,12,13) and, interestingly, also has been implicated in cancer as a 'non-classical oncogene' (14). Importantly, HSF1 activity promotes tumor formation and participates in the maintenance of the transformed phenotype of cancer cells without affecting the viability of normal cells (14). Therefore, HSF1 can function to promote cell survival even under conditions that could potentially become deleterious to cells, such as development of the transformed state.

To further understand HSF1 function during animal development and its role in tumor maintenance, we used RNA aptamer technology as a chemical–genetic approach to inhibit HSF1 activity in *Drosophila melanogaster*. Aptamers are single-stranded RNA molecules that can bind with high affinity to specific molecular surfaces through ionic, hydrophobic and hydrogen bond interactions. They are isolated from combinatorial libraries containing $\sim 1 \times 10^{15}$ different RNA molecules through

*To whom correspondence should be addressed. Tel: +607 255 2442; Fax: +607 255 6249; Email: jtl10@cornell.edu

an iterative process of selection and amplification called systematic evolution of ligands by exponential enrichment (SELEX) (15,16). The large sequence complexity associated with such a starting library enhances the probability of isolating specific and high-affinity aptamer RNAs to various types of molecular targets, ranging from single small molecules (17) to distinct functional domains on a protein (18). Aptamers have also been used previously in therapies (19,20) and in basic research (21,22), demonstrating the broad utility of these molecular inhibitors. Aptamers can not only be selected to bind and inhibit distinct molecular surfaces with high specificity, they can also be expressed *in vivo* under tight genetic control (23) and assert their effect within specific cells, tissues or at specific developmental stages without eliciting an immune response in the targeted organism (24).

Herein, we report the design, construction and validation of a potent inhibitory aptamer RNA molecule for HSF1 (iaRNA^{HSF1}). This iaRNA^{HSF1} contains two HSF1 binding domains engineered from a previously isolated RNA aptamer that targets the highly conserved HSF1 DNA binding domain-linker region (25). In *Drosophila*, we demonstrate that this iaRNA^{HSF1} is highly specific to HSF1 and can interfere with the HSF1 *trans*-activation function under both non-induced and HS conditions *in vivo*. Because of the broad implication of increased Hsp levels in diseases, such as human cancer (14,26–29), we examined the effect of iaRNA^{HSF1} under conditions that model cellular transformation in flies. In *Drosophila*, HSF1 inhibition by iaRNA^{HSF1} suppresses the abnormal phenotypes that are induced by the expression of gain-of-function mutants of the epidermal growth factor receptor (EGFR *ellipse* mutant) and Raf oncogenes, and the effects of iaRNA^{HSF1} expression are similar to the usage of *Hsp83* loss-of-function mutants or treatment of flies with the Hsp83 inhibitor 17-allylamino-17-demethoxygeldanamycin (17-AAG), a frequently used anticancer agent in humans (30).

MATERIALS AND METHODS

Oligonucleotides and other reagents

A single iaRNA^{HSF1} unit was constructed in two parts by extending 50 pmol of each of the following primer sets (I and II; III and IV) in 100 µl using a single round PCR reaction:

(I) 5′-CCGCTCGAGTGACGTTGGCATCGCGATACA AAATTAAGTTGAACGCGAGTTCTTCGGAAT,
(II) 5′-GGCCGGAATTCAAGGAGTATGACGAAGGC AGTTGAATTCCGAAGAACTCGCGTTCAACTT,
(III) 5′-GGCCGGAATTCAACTGCCTTCGGGCATC GCGATACAAAATTAAGTTGAACGCGAGTT CTTGGAGGCTCGACGTCT,
(IV) 5′-CGCGTCGACGTTTCGTCCTCACGGACTC ATCAGTAGCGAAACCACATCGCTAGACGT CGAGCCTCCAAGAACTCG.

Each half of the molecule was purified by running the extended products on high-resolution 8% native gel and extracted from the gel matrix as visualized by EtBr staining. Then each template was restricted with EcoR1 (Invitrogen), ligated together, and cloned into pstBlue-blunt cloning vector (Invitrogen): pstBlue.iaRNA^{HSF1X1} is a coding sequence that contains two individual (AptHSF1-1) gene upstream of a self-cleaving hammer-head ribozyme.

Construction of synthetic genes

Repetitive head-to-tail iaRNA^{HSF1} genes were created by sub-cloning iaRNA^{HSF1X1} into a Gateway donor vector (pDONR221.iaRNA^{HSF1X1}) by lifting the iaRNA^{HSF1X1} sequence from pstBlue.iaRNA^{HSF1X1} using primers containing the AttB1F and AttB2R Gateway cloning sequences (Invitrogen): 5′-AAG TTT GTA CAA AAA AGC AGG CTT CGG ATC CAG AAT TCG TGA TC and 5′-GGG GAC CAC TTT GTA CAA GAA AGC TGG GTT AGC CTA GGT CGA CG. Because each iaRNA^{HSF1} unit is flanked by the complementary asymetric Xho1 and Sal1 restriction sites at the 5′- and 3′-ends, respectively, we can use the general Gateway cloning strategy to select for correctly ligated tandem iaRNA^{HSF1} repeats (Supplementary Methods S1). In this method, a single iaRNA^{HSF1X1} unit is first lifted from pDONR221.iaRNA^{HSF1X1} via PCR and the resulting amplicon is cut with either Sal1 or Xho1 before the cut products are combined and ligated together. Using this scheme, only those products that are in proper head-to-tail orientation contain the required Gateway AttB sites in the 5′- and 3′-ends (AttB1F.iaRNA^{HSF1X2}.AttB2R) needed for creation of an Gateway compatible *Drosophila* transformation expression vector, pUAS.iaRNA^{HSF1X2}. Using the polymer of two as template and repeating the polymerization strategy creates a polymer of four, p{UAS.iaRNA^{HSF1X4}, w+}. Overall, geometric progression of polymeric length is achieved in each subsequent round of polymerization.

Drosophila strains

Parental iaRNA^{HSF1} animals were created by injecting *Drosophila*^{w1118} embryos with p{UAS.iaRNA^{HSF1X8}, w+} and p{UAS.iaRNA^{HSF1X16}, w+} transformation vectors and screening the progeny of F1 females for animals that contain the mini-white gene when crossed to a double-balanced CSX fly line containing CyO(2); TM6(3); Xasta(2,3). Sites of *p*-element insertions were determined genetically by continuous backcrossing to the CSX stock, resulting in homozygous fly lines that contain aptamer genes in various chromosomes: (i) UAS.iaRNA^{HSF1X8}(X), (ii) UAS.iaRNA^{HSF1X16}(X), (iii) UAS.iaRNA^{HSF1X8,16}(X), (iv) UAS.iaRNA^{HSF1X8}(II), (v) UAS.iaRNA^{HSF1X16}(II), (vi) UAS.iaRNA^{HSF1X8,16}(II), (vii) UAS.iaRNA^{HSF1X16}(III). To express iaRNA^{HSF1}, we crossed homozygote UAS.iaRNA^{HSF1} parentals with various Gal4 sources purchased from *Drosophila* Stock Center (Bloomington): 6983 (Salivary Gland Gal4), 5138 (Ubiquitous tubulin Gal4). Systemic iaRNA^{HSF1} expressing animals were created by isolating F1 females from aptamer parentals in the second chromosome (UAS.iaRNA^{HSF18} and UAS.iaRNA^{HSF18,16}) mated to 5138 animals.

Heterozygote F1 males were then mated to CSX females, and the resulting F2 animals that contained both aptamer genes and Gal4 protein (UAS.iaRNA^{HSF1}/CyO; Tub.Gal4/Sb) were isolated and isogenized to create true breeding aptamer expressing lines. Other Bloomington stocks used in this study include: 5693 (Hsp83^{e6D} antimorphic mutant), 5743 (Duplication 61F7–F8; 64B10–12). Animals containing the pUAS.eGFP(I) transgenes were a kind gift provided by Dr Garcia-Bellido's laboratory, and animals expressing the gain of functions EGFr^{Elp} and Raf^{BT98} mutants were kindly provided by Dr Marc Therrien's laboratory.

In vitro binding assays

Internally labeled ^{32}P-UTP iaRNA^{HSF1} was transcribed from an iaRNA^{HSF1X1} PCR template containing a 5′-T7 promoter using Maxi-script Kit and instructions (Ambion) and purified by gel electrophoresis. Electrophoretic motility shift assays (EMSA) were performed by addition of increasing molar amounts of purified GST-HSF1 protein to limiting amounts of ^{32}P-iaRNA^{HSF1} (<1 nM) using the following binding conditions: 25 mM Tris–HCl, 75 mM KOAc, 0.5 Mm $MgCl_2$, 10% glycerol pH 7.4 and allowing complexes to form for 0.5 h at 25°C. The RNA protein complexes were separated in 6% native gel (3 mM Tris–HCl, 200 mM glycine, 0.5 mM $MgCl_2$). Competition experiments were performed by pre-incubating increasing molar amounts of cold-iaRNA^{HSF1} mixed with T4 kinase labeled Hsp83 or Hsp70 promoter DNAs to 50 nM purified GST-HSF1 before separating the complexes on 2% native gels (0.5× TAE, 0.5 mM $MgCl_2$) or by filter binding assays. The promoter DNA sequences were amplified from *Drosophila* genomic DNA using the following primer sequences:

Hsp83−449F: 5′-ACTTGACTGGGCTTGTAGCAGGTT,
Hsp83+114R: 5′-TTCTGGATGCCAGGGATGCAACTT,
Hsp70−200F: 5′-TGCCAGAAAGAAAACTCGAGAAA,
Hsp70+64R: 5′-CTGCGCTTGTTTGTTTGCTTAGCT.

RNA quantification

Total RNA was extracted from whole animals using Trizol reagent (Invitrogen). Quantification of the relative transcript levels was determined by oligo-dT reverse transcription, followed by real-time PCR analysis (RT–qPCR) using the following primer sets:

Rp49+141F: 5′-CCCAAGGGTATCGACAACAGA,
Rp49+204R: 5′-CGATGTTGGGCATCAGATACTG,
18 S+417F: 5′-TGACGAAAAATAACAATACAGGAC TCA,
18S+569R: 5′-CAGACTTGCCCTCCAATTGG,
iaRNA^{HSF1} F: 5′-TGGTTTCGCTACTGATGAGTCCGT,
iaRNA^{HSF1} R: 5′-GCAGTTGAATTCCGAAGAACTCGC,
Hsp70Ab+2155F: GGTCGACTAAGGCCAAAGAGTCTA,
Hsp70Ab+2266R: TCGATCGAAACATTCTTATCAGT CTCA,
Hsp83+3628F: 5′-GCGACCAGTCGAAACAAACAACCA,
Hsp83+3732F: 5′-AACTCGGCCGTAGTAAACTCAG,
Hsp26+580F 5′-CAAGGTTCCCGATGGCTACA,
Hsp26+667R 5′-CTGCGGCTTGGGAATACTGA.

All statistical analyses in this study were calculated using Student's *t*-test.

Immunofluorescent assays of polytene chromosomes

Salivary glands were dissected from third stage instar larvae in 0.5× Grace's medium. Chromosomes were spread, fixed onto slides and immunostained using antibodies targeting HSF1, GAGA factor (GAF) as described previously in Schwartz *et al.* (31).

Morphological studies

Aptamer expressing animals were scored for phenotypic abnormalities using a dissecting microscope. Here, the abnormal *Drosophila* traits were quantified by screening a population of aptamer expressing animals (>500 flies) and determining the number of animals with abnormal traits in the total population. Pictures were taken using an 8.0 Mb Nikon digital camera mounted onto the microscope. Quantification of morphological abnormalities was calculated by quantifying abnormal size or area using the ImageJ software.

Cell culture

iaRNA^{HSF1X8} was subcloned into Gateway pDEST48 (Invitrogen) and stable *Drosophila* S2 cells were selected by maintaining cells in 6 μg/ml Blasticidin reagent. iaRNA^{HSF1} was induced using 0.5 mM $CuSO_4$. iaRNA^{HSF1} half-life ($t_{1/2}$) determination was performed by treating cells with 0.5 mM $CuSO_4$ for 24 h before adding 1 μg/ml alpha-amanitin, a potent RNA Pol II inhibitor. Upon the addition of amanitin, cells were collected and the total RNA samples were isolated using the Trizol reagent and protocol. Total iaRNA^{HSF1} values were calculated by comparing their relative levels to 18S RNA levels at specific time points following amanitin treatment.

RNAi treatment

Approximately 1×10^6 *Drosophila* S2 cells were incubated with 10 μg dsRNA targeting HSF1 and Hsp83 for 5 days using genes containing T7 promoter targeting each sequence amplified from *Drosophila* genomic DNA:

T7Hsp83+378F: 5′-TAATACGACTCACTATAGGGTT CCATGATCGGTCAGTTCGGTGT,
T7Hsp83−1048R: 5′-TAATACGACTCACTATAGGGC GTACAGCTTGATGTTGTTGCGCT,
T7HSF1 F: 5′-GAATTAATACGACTCACTATAGGG AGAGCCTTCCAGGAGAATGCA,
T7HSF1R: 5′-GAATTAATACGACTCACTATAGGG AGAGCTCGTGGATAACCGGTC.

RESULTS

Design, construction and validation of the iaRNA^{HSF1} expression system

Previously, we isolated an RNA aptamer that binds the DNA binding domain of *Drosophila* HSF1 with an apparent dissociation constant (K_d) of 20–40 nM (25). Because HSF1 is multimeric, we used this aptamer to construct a divalent version that we demonstrate has a several fold higher affinity, $K_d \sim 8$ nM (Figure 1A–C). This improved avidity of iaRNA^{HSF1} is sufficient to prevent HSF1 from binding to its natural binding sites on the *Hsp70* and *Hsp83* promoters *in vitro* (Figure 1D and E). As shown here, increasing the concentrations of HSF1 results in the formation of various protein–DNA complexes as visualized by the altered electrophoretic motility (Figure 1D, lanes 2–4). The long HS element (HSE) of *Hsp83* can bind multiple HSF1 trimers, and the weaker bands of intermediate mobility likely represent binding of non-saturating amounts HSF1 trimers to this HSE. These weaker bands and the major shifted band are all effectively inhibited by increasing amounts of iaRNA^{HSF1} (Figure 1D, compare lanes 5–8 versus 9–12).

To test the effect of iaRNA^{HSF1} on HSF1 function in animals, we generated an aptamer expression system designed to rapidly produce high levels of nuclear localized dimeric iaRNA^{HSF1} in desired cell types. The approach was a systematic step-wise variation of that used by Shi *et al.* (23). The dimeric iaRNA^{HSF} was joined to a hammerhead ribozyme and this unit was duplicated and the product reduplicated by a forced-Gateway cloning strategy to generate up to 16 repetitive head-to-tail repeats under the control of a Gal4-activated promoter (Figure 2A and Supplementary Methods S1). The resulting expression system allows high-level expression of dimeric aptamer RNAs, because each repeating aptamer coding unit within a given polymeric template is flanked by a self-cleaving hammer-head ribozyme. Upon transcription of the polymeric template RNA in a tissue expressing the Gal4 transcription activator, the hammer-head ribozymes undergo self-cleavage resulting in the release of multiple free functional iaRNAs from every transcription cycle (23) (Supplementary Figure S1A). This self-cleavage ensures that the aptamer RNAs are not polyadenylated and not substrates for nuclear export; therefore, they should remain localized within the nucleus. Additionally, the self-ligation activity of the released form of the hammerhead creates covalently closed circles that are thought to stabilize and protect the RNA aptamer from degradation (23).

To test the stability of iaRNA^{HSF1} in living cells, we analyzed the rate of iaRNA^{HSF1} decay in stable *Drosophila* cells at specific times following alpha-amanitin treatment. In these experiments, the iaRNA^{HSF1} exhibited an *in vivo* half life of ~2 h (Supplementary Figure S1B).

Finally, to test the production of iaRNA^{HSF1} in whole *Drosophila* animals, we crossed flies with the Gal4-regulated polymeric aptamer gene with a line expressing a tubulin-promoter-driven Gal4 gene. The iaRNA^{HSF1} level is elevated ~150-fold over parental strains that lack Gal4 protein (Supplementary Figure S1C) demonstrating that the aptamer gene is regulated by Gal4. Collectively, our results reveal that this engineered polymeric dimeric aptamer construct has an improved apparent affinity for HSF1, is stable under cellular conditions, and can be effectively induced to high levels *in vivo*.

iaRNA^{HSF1} is a potent HSF1 antagonist under non-heat shock conditions

To determine the *in vivo* efficacy of the iaRNA^{HSF1} as a HSF1 antagonist, we measured its effect on known HSF1 gene targets under both non-heat shock (NHS) and HS conditions. We focused initially on the *Hsp83* gene locus (63B), which is the ortholog of mammalian *Hsp90*, because it is expressed under non-stress inducing conditions, and HSF1 is significantly enriched at this locus compared to other loci (32,33). We investigated the effects of iaRNA^{HSF1} expression at three different levels: (i) HSF1 binding to the *Hsp83* chromosomal locus, (ii) Hsp83 mRNA levels and (iii) traits in animals. Antibody staining for HSF1 on *Drosophila* salivary gland chromosomes confirms that under normal growth conditions HSF1 preferentially binds to the *Hsp83* gene locus (63B) [Figure 2B, compare HSF1 signal (red) relative to GAF control (green)]. However, upon iaRNA^{HSF1} expression, the HSF1 levels at the 63B locus is significantly reduced by ~50% ($P = 0.035$) (Figure 2C, left).

Previous reports have implicated the enhancer elements and upstream regulatory sequences present in the promoter regions of the *Hsp83* gene as being critical for *Hsp83* gene expression (34); however the *Hsp83* upstream region also has a tandem array of nine binding sites for the HSF DBD. Because, there is currently no direct evidence indicating whether HSF1 has a role in regulating the basal expression of *Hsp83*, we tested whether HSF1 inhibition compromises *Hsp83* expression levels by quantifying the levels of *Hsp83* mRNA in iaRNA^{HSF1} expressing and wild-type (Gal4 parental) animals not exposed to thermal stress (NHS). In these and the following RT–qPCR experiments, we determine and compare HS mRNAs by normalizing their values to a housekeeping gene whose level does not vary relative to total RNA in response to HSF1 aptamer expression, HSF1 RNAi treatment, or temperature. Here, animals that express iaRNA^{HSF1} contain an ~50% reduction of *Hsp83* mRNAs compared to control animals (Figure 2C, right) ($P = 0.008$), indicating that under non-HS conditions HSF1 activity is required for the expression of *Hsp83*. We confirmed this result using another approach, which involved RNAi-depletion of HSF1 from *Drosophila* S2 cells. In these experiments, HSF1 knockdown resembled the effects of iaRNA^{HSF1} expression and similarly reduced the expression levels of *Hsp83* and *Hsp70* transcripts (Supplementary Figure S1D), thus further demonstrating that normal HSF1 activity is required for the full expression of HS mRNAs under normal growth conditions.

Adult animals that constitutively express iaRNA^{HSF1} display phenotypic abnormalities in the abdominal segments, wing shape and morphology, bristles and eye

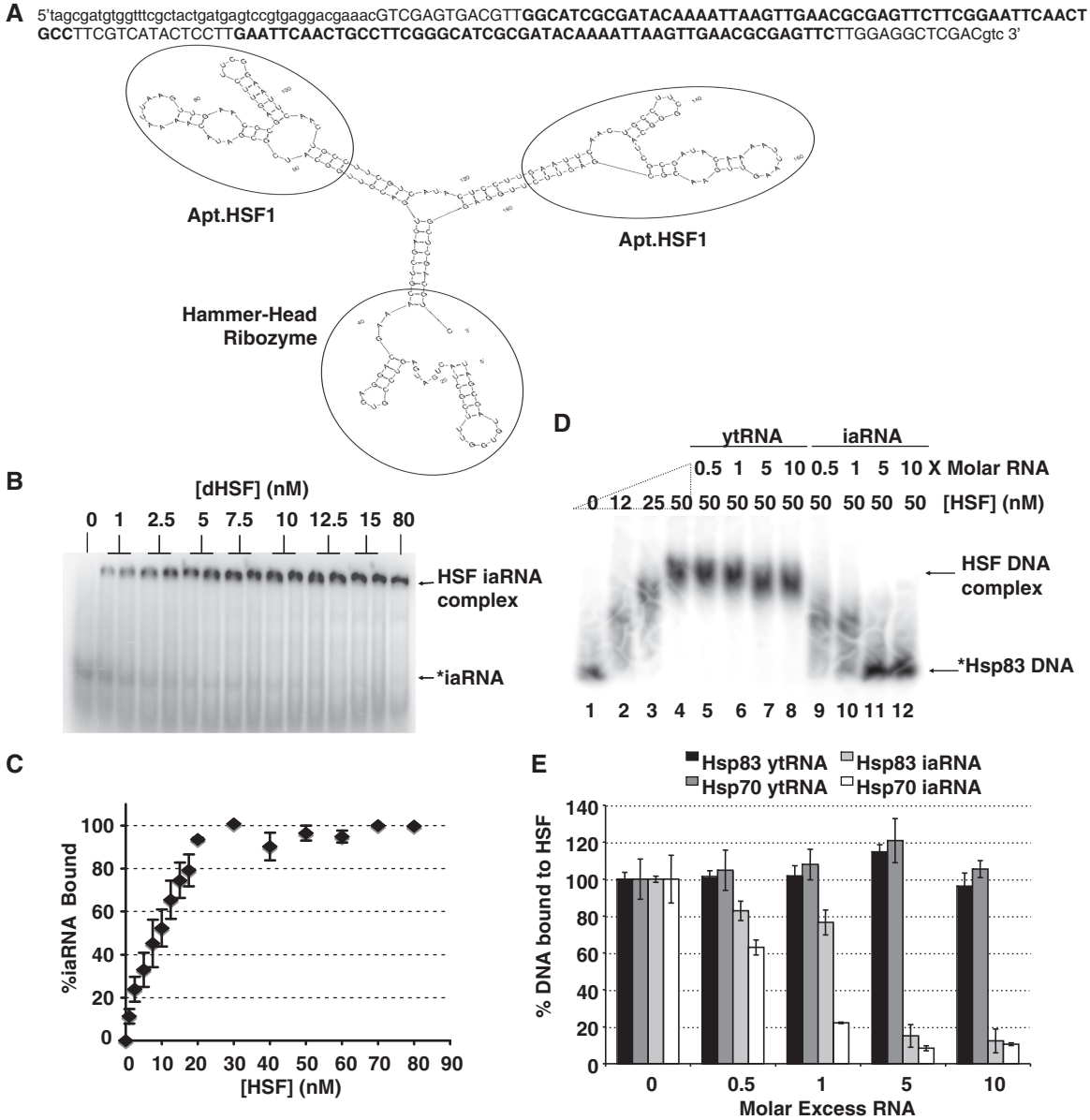

Figure 1. Biochemical characterization of an inhibitory aptamer that targets HSF1, iaRNA^{HSF1}. (**A**) Lowest energy diagram predicting the secondary structure of the dimeric HSF aptamer (iaRNA^{HSF1}) using M-fold (upper case = HSF1 aptamer; lower case = self-cleaving hammer head ribozyme). (**B**) Electrophoretic motility shift assay (EMSA) using radiolabeled iaRNA^{HSF1} (1 nM) and increasing amounts of dHSF1 protein shows that the aptamer RNA binds to its target avidly. (**C**) Quantification of independent EMSA assays reveals the apparent affinity of the iaRNA^{HSF1} $\sim K_d = 8$ nM ($n = 5$, error indicates %SEM). (**D**) iaRNA^{HSF} competes with HSF1 DNA binding at native promoters *in vitro*. HSF1 EMSA using limiting amounts of Hsp83 promoter DNA (1 nM) (−449 > +114)(lanes 2–12), and increasing molar (*M*) concentrations of cold 'non-radiolabeled' iaRNA^{HSF1} (lanes 9–12) or yeast tRNA (lanes 5–8). (**E**) Quantification of competition experiments by filter binding assays using Hsp83 (−449 > +114) or Hsp70 (−200 > +64) promoter DNA. Data normalized to highest ytRNA signal (Hsp70 %SEM $n = 3$, Hsp83 %SEM $n = 6$).

protrusions in specific genetic backgrounds at high frequencies (Figure 2D). Intriguingly, the aptamer-induced phenotypes closely resemble the abnormalities that occur when Hsp83 activity is reduced; although the developmental defects occur at much greater frequencies (35,36). This increased penetrance is best illustrated by the notched wing phenotype observed in ~90% of iaRNA^{HSF1} expressing animals; while this same phenotype is only present in ~5–20% of the wild-type animals that have been raised in media containing the Hsp83 inhibitor (17-AAG) during the first two generations, and in <1% of *Hsp83^{e6D}* antimorphic mutants. The observed increased penetrance of abnormal traits that occurs among aptamer expressing animals might be a result of inbreeding of fly populations that have such abnormal traits, as has been shown in previous studies of *Hsp83* mutant animals or feeding animals with 17-AAG (36). Additionally, or alternatively, we cannot rule out HSF1 having some contribution to basal expression of other HS proteins that are known to contribute to Hsp83's

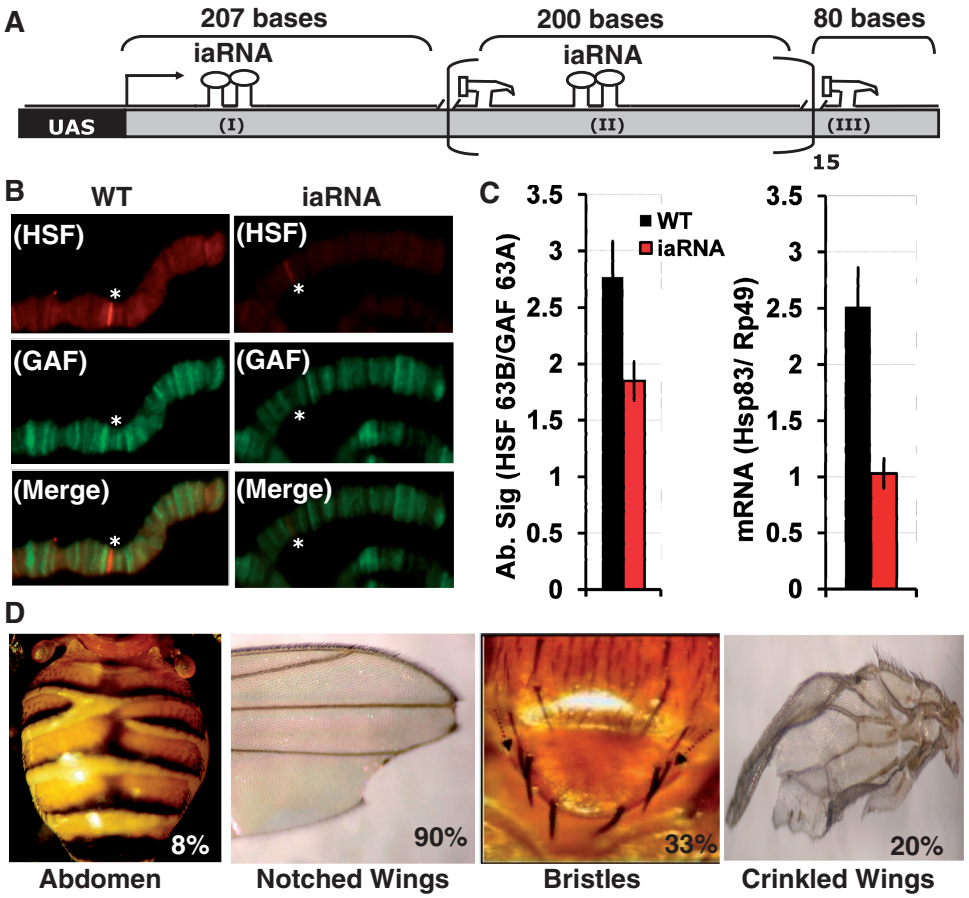

Figure 2. iaRNA^{HSF1} is a potent HSF1 antagonist under NHS conditions. (**A**) Design of iaRNA expression system *in vivo*. Diagram of a polymeric template of 16 iaRNA^{HSF1} gene units and their corresponding transcripts (i) corresponds to the first processed iaRNA^{HSF1} which lacks a hammerhead, (ii) correspond to the middle iaRNA^{HSF1} repeats that contain the 'self-cleaving' hammer head ribozymes and (iii) corresponds to the final processed hammer head ribozyme that does not have the iaRNA^{HSF1}. (**B**) Constitutive iaRNA^{HSF1} expression results in decreased HSF1 binding to Hsp83 gene (63B locus) during non-induced (NHS) conditions (note: the average diameter of a polytene chromosome is 4 μm). (**C**) Quantification of the relative intensities shown in panel B among WT (n = 29) and iaRNA^{HSF1} expressing animals (n = 29) (left), and quantification of Hsp83 mRNAs in WT (n = 6) and iaRNA^{HSF1} (n = 6) expressing animals (right) shows that constitutive iaRNA^{HSF1} expression inhibits HSF1 binding to the Hsp83 locus under NHS conditions *in vivo* (observed signals normalized to GAF intensities at 63A). (**D**) HSF1 inhibition by iaRNA^{HSF1} results in adult animals that resemble Hsp83 loss-of-function mutants, and in animals that display abnormal animal morphology within abdominal segments, wings and bristle structures at high frequencies (n >500 animals).

chaperone functions. Taken together, our findings demonstrate that under NHS conditions, iaRNA^{HSF1} expression can compromise HSF1 binding to its native binding sites, such as the *Hsp83* locus (63B), resulting in decreased *Hsp83* transcript levels and giving rise to animals with phenotypes that resemble loss of function *Hsp83* mutants (Figure 2).

iaRNA^{HSF1} is a potent HSF1 antagonist under HS conditions

It is well documented that under HS conditions, HSF1 undergoes homo-trimerization and binds with high affinity to the HS elements (HSE) of HS promoters (33,37). HSF1 binding to promoters results in the recruitment of various components of the transcription machinery (38), dramatic changes in chromatin architecture and nucleosome disruptions over the entire gene locus (39), and ~200-fold increase in expression of major HS genes. Although iaRNA^{HSF1} is predicted to have more difficulty competing against the DNA binding capacity of HS-activated HSF1 homotrimers, we do observe a modest but reproducible inhibitory effect. Figure 3A shows that fly lines that contain 48 dimeric aptamer repeats (three 16-mer arrays inserts crossed into a single line) have high-level iaRNA^{HSF1X48} expression that is sufficient enough to compromise HSF1 binding to the *Hsp70* (87A and C) loci following HS treatment. Quantification of the HSF1 antibody signals, which are normalized to GAGA factor antibody staining at a nearby site that does not undergo 'puffing' (86E), shows the effectiveness of the iaRNA^{HSF1} at inhibiting the ability of HSF1 to bind at both the 87A and 87C loci (Figure 3B). Furthermore, quantification of the total mRNAs from three major classes of HS genes: *Hsp26*, *Hsp70* and *Hsp83* demonstrates that iaRNA^{HSF1} expression reduces their expression (Figure 3C).

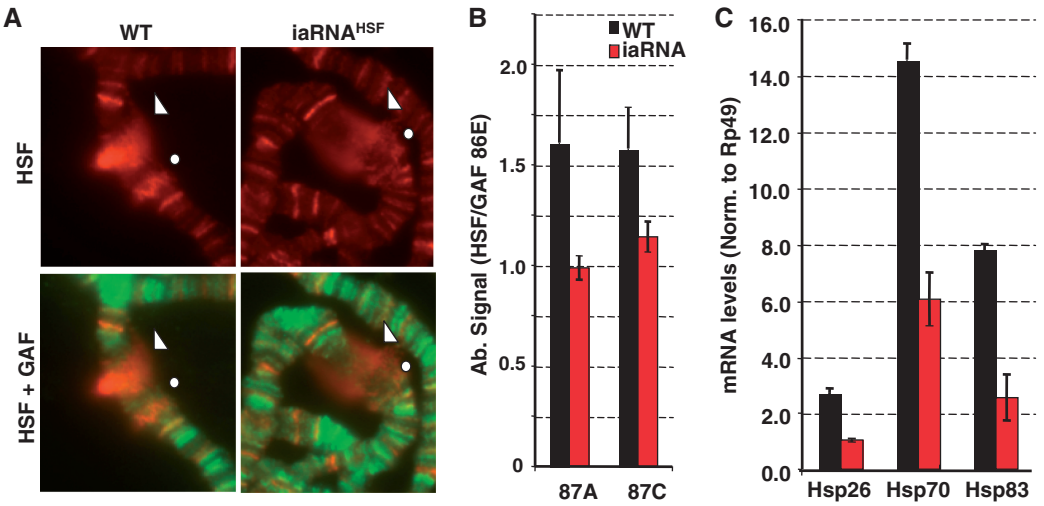

Figure 3. iaRNA^{HSF1} expression inhibits HSF1 activity under HS conditions *in vivo*. (**A**) High-level iaRNA^{HSF1} inhibits HSF1 binding to *Hsp70* gene loci under HS conditions (left column = WT, right column = iaRNA^{HSF1X48}; antibodies: red = HSF1, green = GAF, blue = DNA, dot = 87A locus, triangle = 87C locus) (note: the average diameter of a polytene chromosome is 4 μm). (**B**) Quantification of the relative fluorescence of HSF1 in panel E at *Hsp70* (87AC loci) among WT or iaRNA^{HSF1X48} expressing animals (signals normalized to GAF intensity at 86E locus. WT $n = 5$; iaRNA^{HSF1} $n = 14$). (**C**) Constitutive iaRNA^{HSF1} expressing compromises major HS gene activation by HSF1 during heat stress (mRNAs quantified by RT–qPCR. Error %SEM, WT $n = 4$, iaRNA^{HSF1} $n = 4$).

Functional specificity of the *in vivo* iaRNA^{HSF1}–HSF1 interaction

Overexpression of either iaRNA^{HSF1} or HSF1 results in increased lethality and an increased frequency of specific morphological phenotypes. To assess the specificity of iaRNA^{HSF1} for HSF1, we reasoned that overexpression of both molecules within the same animal should ameliorate the aberrant phenotypes of each. This genetic approach is analogous to factor titration or add-back experiments in biochemical assays, where the inhibition of a protein by an RNA aptamer is reversed by the addition of excess protein (22,23,25).

First, we assessed if HSF1 overexpression could suppress the abnormalities induced by iaRNA^{HSF1} overexpression. Here, systemic iaRNA^{HSF1} expression results in lethality that occurs with increasing iaRNA^{HSF1} gene dosage (Figure 4A, compare animals that express 8, 24 and 48 iaRNA^{HSF1} repeats). We reasoned that the observed lethality that occurs among animals expressing high levels of iaRNA^{HSF1X48} is likely due to the fact that HSF1 is an essential gene for *Drosophila* development (9). This iaRNA^{HSF1}-induced effect is effectively suppressed upon HSF1 co-expression (Figure 4A, compare gray and blue column). Additionally, we took advantage of the abnormal wing (notching) defect that occurs with a high frequency in iaRNA^{HSF1} expressing animals to further determine the specificity of iaRNA^{HSF1} to HSF1. We choose to focus on the abnormal (notch) wing phenotype because it occurred most frequently in the aptamer expressing population, and as with any genetic suppression analysis, it provided us with an easily observable phenotype that was quick to score. Figure 4B shows that the notched wing defect occurs in iaRNA^{HSF1} expressing animals and is absent in any of the parental stocks (Figure 4B, compare parental controls). Moreover, this abnormality is not affected by GFP overexpression, but it is effectively rescued upon overexpression of either HSF1, or Hsp83, a major product of HSF1 activity in non-stressed cells (Figure 4B).

Second (a complementary test), we assayed if iaRNA^{HSF1} expression could suppress the abnormalities induced by HSF1 overexpression. We find that tissue-specific HSF1 overexpression results in abnormally small salivary glands (Figure 4C, compare right and left panel). This abnormality is effectively suppressed when iaRNA^{HSF1} co-expressed with overexpressed HSF1 (Figure 4C, middle panel). Quantification of the salivary gland length among WT animals and animals that either overexpress HSF1 alone or with iaRNA^{HSF1} shows that iaRNA^{HSF1} co-expression restores the salivary gland morphology to nearly WT size (Figure 4D). Furthermore, we find that the high frequencies of lethality in flies with high-level systemic HSF1 overexpression (Figure 4A) is effectively suppressed by iaRNA^{HSF1} co-expression, resulting in viable and fertile animals (Figure 4A). Lastly, we decided to express the HSF1 aptamer (iaRNA^{HSF1}) and compare its effects with a control aptamer RNA (Rev) that lacks the sequence specificity to target HSF1 protein in stably selected *Drosophila* S2 cells. Placing each aptamer gene under the control of the copper-inducible promoter results in tight chemical control and high amounts of aptamer levels upon addition of low amounts of $CuSO_4$ (Supplementary Figure S2A). In this system, we observe decreased HSF1 levels at the *Hsp70* promoter upon iaRNA^{HSF1}, but not control RNA (Rev) expression (Supplementary Figure S2B). Moreover, iaRNA^{HSF1} expression inhibits $CuSO_4$ induction of *Hsp70* while expression of the control RNA sequence does not (Supplementary Figure S2C).

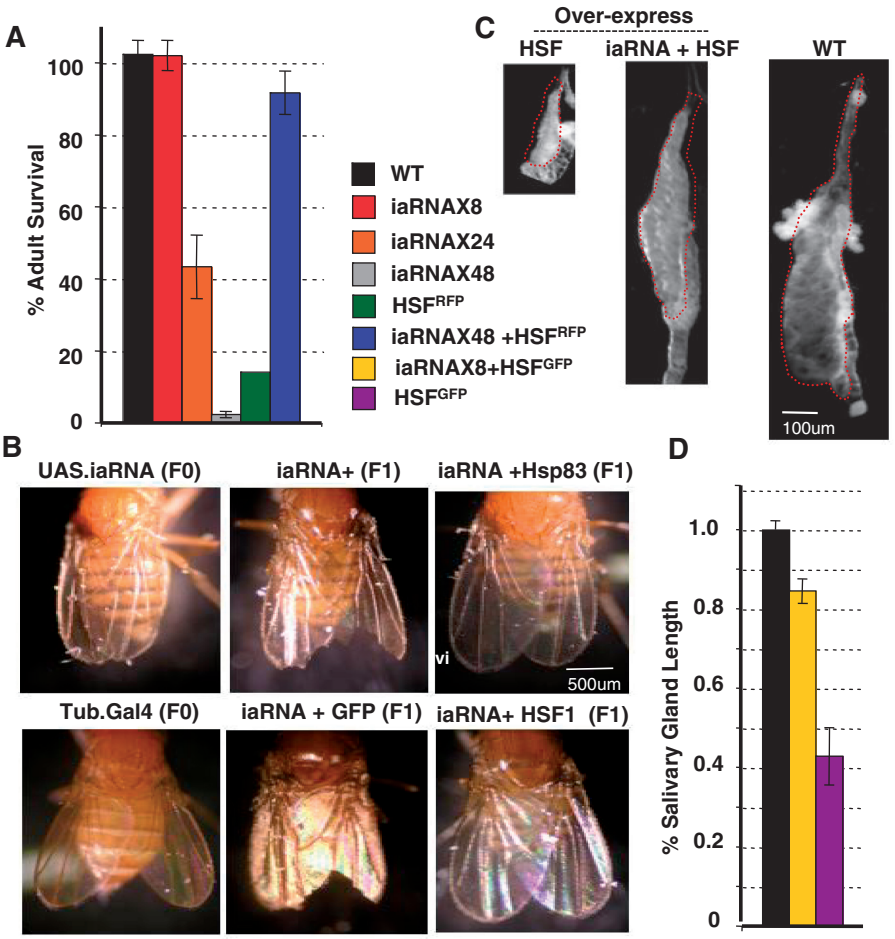

Figure 4. iaRNA^{HSF1} inhibits HSF1 with high specificity *in vivo*. (**A**) Co-expression of iaRNA^{HSF1} and HSF1 suppress the lethality induced by either high-level iaRNA^{HSF1} or HSF1 overexpression. (**B**) HSF1 and Hsp83 overexpression, but not GFP overexpression, completely suppresses the notched wing phenotype induced by high-level iaRNA^{HSF1} expression [WT parental controls: (F0) UAS.iaRNA^{HSF1} and Tubulin Gal4 stocks], iaRNA^{HSF1} expressing animals with notched wings (F1: iaRNA^{HSF1}), iaRNA^{HSF1} expressing animals that overexpress GFP protein (F1: iaRNA^{HSF1} + GFP), iaRNA^{HSF1} expressing animals with an additional copy of *Hsp83* gene (F1: iaRNA^{HSF1} + *Hsp83*), and animals that overexpress iaRNA^{HSF1} and HSF1 protein (F1: iaRNA^{HSF1} + HSF1) ($n > 500$ animals). (**C**) iaRNA^{HSF1} suppresses the adverse effects of HSF1 overexpression in the *Drosophila* salivary glands (left = overexpress HSF1^{GFP}; middle = overexpress HSF1^{GFP} + iaRNA; right = WT). (**D**) Quantification of salivary gland length of panel C (error %SEM, WT $n = 9$; HSF1^{GFP} $n = 8$; HSF1^{GFP} + iaRNA^{HSF1} $n = 15$).

Taken together, we conclude that iaRNA^{HSF1} does not produce its phenotypes non-specifically, but rather acts on the intended target, HSF1, thereby inhibiting expression of Hsp83, which is HSF1's primary target of binding and regulation under non-induced conditions.

iaRNA^{HSF1} expression attenuates phenotypes of hyperactive mutations in the MAPK signaling pathway

Hsp83 is known to modulate the MAPK signaling pathway, a well-conserved and important regulatory pathway that is frequently overactivated in human cancers (40). In *Drosophila*, gain-of-function mutations within the MAPK pathway does not result in tumor formation; rather, hyper-activation of the MAPK pathway results in an altered cell fate specification and abnormal tissue morphology. Components of this pathway, such as the EGFR and Raf oncogenes, depend on normal levels of Hsp83 activity for their proper folding, localization or kinase activity (1,41). Thus, the inhibitory potential of the aptamer on the MAPK pathway can be analyzed *in vivo* by comparing the effects of iaRNA^{HSF1} expression in animals that also harbor gain-of-function EGFR (*ellipse*) or Raf (*Raf^{BT98}*) mutations. Here, tissues that have decreased MAPK signaling activity should more closely resemble the tissues of animals that do not harbor the gain-of-function mutants.

Expression of iaRNA^{HSF1} inhibits HSF1 and this, in turn, decreases Hsp83 levels. Because Hsp83 is needed for MAP kinase pathway function, we sought to determine if iaRNA^{HSF1} expression might suppresses the abnormalities induced by gain-of-function mutations of the *Drosophila EGFR^{ellipse}* and *Raf^{BT98}* oncogenes. Heterozygote animals that express *EGFR^{ellipse}* have been previously shown to contain abnormal wing veins morphology (42). Indeed, this abnormality is effectively

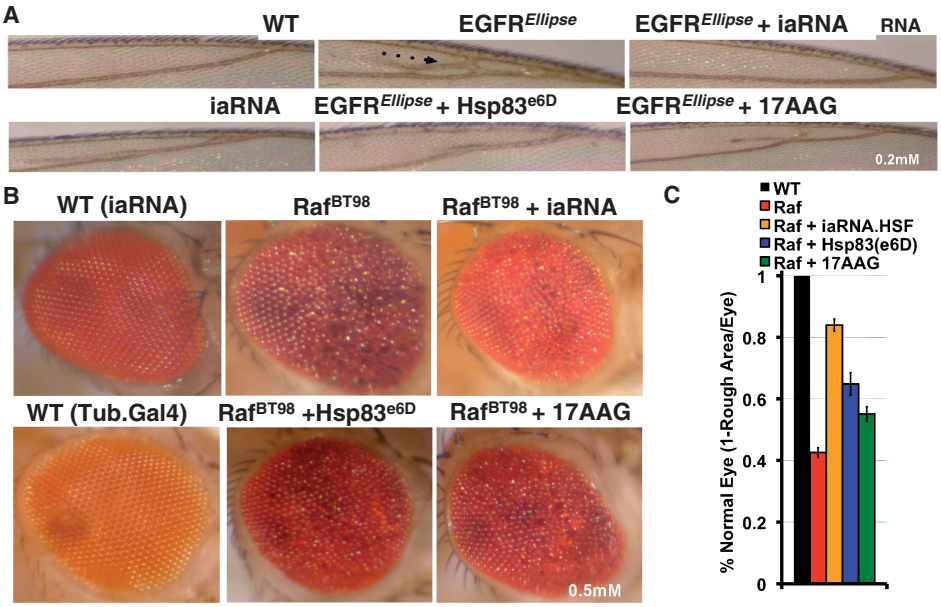

Figure 5. Expression of iaRNA^{HSF1} suppresses gain-of-function mutations of genes in the MAPK signaling pathway. (**A**) iaRNA^{HSF1} expression and Hsp83 inhibition suppress the abnormal wing phenotype induced by the EGFr^{Elp} mutant. (**B**) iaRNA^{HSF1} expression and Hsp83 inhibition suppress the rough eye phenotype induced by activated Raf^{BT98} mutant. (**C**) Quantification of rough eye phenotypes in panel B calculated by area. Error %SEM, WT (n = 5); Raf^{BT98} (n = 26); Raf^{BT98} + iaRNA^{HSF1} (n = 33); Raf^{BT98} + Hsp83^{e6D} (n = 33); Raf^{BT98} + 3.6 μM 17AAG (n = 33).

suppressed when HSF1 is inhibited by iaRNA^{HSF1}, or when Hsp83 activity is compromised by expression of the *Hsp83^{e6D}* antimorphic mutant or when *EGFR^{ellipse}* hemizygote flies are treated with the Hsp90 inhibitor 17-AAG (Figure 5A).

Similarly, heterozygote animals that express a gain-of-function *Raf^{BT98}* protein have been shown to contain multiple cells within each ommatidium resulting in flies with a distinct rough eye morphology (Figure 5B). Moreover, it has been previously demonstrated that *Raf^{BT98}* mutants require normal Hsp83 activity to exert this eye specific defect (41). In agreement with the previous findings, we find that the rough eye phenotype that is induced by *Raf^{BT98}* expression can be reversed by reducing Hsp83 activity through the co-expression of the *Hsp83^{e6D}* antimorphic mutant, or by treating *Raf^{BT98}* animals with 17-AAG (Figure 5B). Consistent with our findings that HSF1 controls the expression of Hsp83, we find that HSF1 inhibition by the aptamer also results in the strong suppression of the rough eye phenotype that is caused by increased *Raf^{BT98}* signaling activity (Figure 5B). The affected surface area of the eye with a rough eye phenotype in each of these overactive MAPK signaling genetic backgrounds can be effectively attenuated by iaRNA^{HSF1} expression or direct Hsp83 inhibition (Figure 5C).

DISCUSSION

iaRNA^{HSF1} is a novel HSF1 DNA binding domain inhibitor *in vitro* and *in vivo*

In this study, we describe the *in vivo* utility of an aptamer that targets the highly conserved HSF1 DNA binding domain. We engineered a potent inhibitor of trimeric HSF1 by constructing a dimeric molecule derived from two copies of a previously selected RNA aptamer, which had a modest K_d of ~20–30 nM. The dimeric aptamer (iaRNA^{HSF1}) binds HSF1 with an improved affinity of K_d of ~8 nM. By creating a genetically controlled expression system, which contains polymers of a dimeric aptamer fused to a self-cleaving ribozyme, we demonstrate that we can express iaRNA^{HSF1} at high levels in whole animals. In cells, this RNA molecule displays an *in vivo* half-life of 2–4 h, is adequate to produce the phenotypes in animals seen here. Moreover, it can be a useful inhibitor particularly in basic studies of the HS response that are often performed within the first few hours following stress induction. We do, however, acknowledge that the effectiveness of the aptamer could benefit from other modifications that further limit exonuclease degradation.

It is well-documented that HS stress can affect the monomer–oligomer equilibrium status of HSF1 (43). Within seconds following a heat stress, HSF1 shifts from a monomer to a homotrimer state, binding stably and cooperatively to HS gene promoters (37). This can be visualized *in vivo* using real-time imaging techniques; under normal growth conditions, where monomeric HSF1 displays rapid off-rates with its target genes, but is stably associated with target loci after the cells have been exposed to heat stress (33). Here, we show that our HSF1 aptamer can prevent HSF1 binding to HS loci and its ability to induce gene expression under both normal and stress conditions *in vivo*. While the aptamer is effective in inhibiting the modest HSF1 DNA binding activity in NHS cells, it only partially inhibits strong HSF1 binding

in HS cells (Figure 3). We note that aptamer expressing animals show normal survival after heat stress, presumably because the levels of chaperone expression is sufficient to overcome the proteotoxic effects of heat. However, high-level expression of this aptamer in yeast cells results in strong growth defects at elevated temperatures (44).

Whenever a ligand such as an aptamer is used *in vivo* to study and manipulate the function of a protein, it is important to know whether the intended target is specifically recognized by the ligand/drug. However, testing the binding of iaRNA^{HSF1} to every protein in a cell is not feasible. Instead, we use functional assays to demonstrate that effect of iaRNA^{HSF1} is specific to HSF1. The abnormalities that arise from the expression of iaRNA^{HSF1} in *Drosophila* are effectively suppressed by HSF1 co-expression and not a control protein like GFP, suggesting that the aptamer is exerting its effects by targeting HSF1[25]. Conversely, the abnormalities observed in *Drosophila* induced by HSF1 overexpression are also effectively suppressed by iaRNA^{HSF1} overexpression. Moreover, in *Drosophila* S2 cells iaRNA^{HSF1} expression effectively attenuates HSF1 activity while expression of a control aptamer sequence (Rev) does not. Collectively, our analysis provides further supporting evidence for the specific nature of the aptamer–HSF1 interaction *in vivo*.

HSF1 regulates the activity of the Hsp83 (Hsp90) buffering system that promotes adaptation to stress

In contrast to mammals, where the *Hsp83* locus (*Hsp90*) is not controlled by HSF1 but rather by other HSF isoforms (45), here we show that *Drosophila,* which has a single of HSF gene, requires HSF1 for the proper expression of Hsp83 during development. The constitutive level of Hsp83 protein is impressive, reaching concentrations of 1–2% of the total protein content *in vivo* (45–47). This HSF1 involvement in constitutive expression of Hsp83 was first suggested by the fact that the *Hsp83* locus (cytological site 63B) shows the highest HSF1 occupancy over any site on *Drosophila* chromosomes. We also find that either iaRNA^{HSF1} or HSF1 RNAi expression in *Drosophila* reduces the levels of HS transcripts, and in particular, the constitutive levels of *Hsp83*. Hsp83 has a general role in biological processes such as spermatogenesis, protein trafficking, signal transduction, cytoskelletal organization and cell survival pathways (41,48–52). Given the fact that Hsp83 exerts its chaperone functions in concert with other HS proteins; it is, therefore, likely that decreasing various HS mRNAs levels with iaRNA^{HSF1} expression attenuates Hsp83 activity resulting in animals that have phenotypes of previously reported *Hsp83* mutants (35), albeit at much higher frequencies than seen previously in Hsp83 hemizygotes. Moreover, we find that iaRNA^{HSF1} expression effectively attenuates the abnormal activities of Hsp83 client proteins, EGFR and Raf oncoproteins. Collectively, our data suggest that in *Drosophila* the *Hsp83* gene is a primary target of HSF1 regulation during normal conditions, and is highly responsive to HSF1 inhibition during animal development.

This study builds upon a previous *Hsp83*-directed chaparone 'buffering' model (35,36), and our data supports the hypothesis that the master regulator HSF1 is critical for constitutive expression of molecular chaperones. In particular, HSF1 inhibition results in an altered chaperone-driven buffering system that promotes animal trait variation and the signaling activities of cancer causing mutations (Supplementary Figure S3). Herein, we provide an *in vivo* approach aimed at understanding HSF1 function during animal development and its putative role for early drug target validation. Because the HSF1 DNA-Linker domain is highly conserved among eukaryotes (53), it is likely that this novel HSF1 inhibitor (iaRNA^{HSF1}), or derivatives thereof will prove to be a useful reagent(s) that will further aid in unraveling the functions of related HS transcription factors in other model organisms or of HSF1-dependent diseases such as cancer.

SUPPLEMENTARY DATA

Supplementary Data are available at NAR Online.

ACKNOWLEDGEMENTS

The authors would like to thank all members of the Lis and W. Lee Kraus Labs for their helpful suggestions, and, in particular, A. Sevillimedu for helpful discussions; and Madam J. Werner for performing the polytene chromosome spreads. The authors would also like to thank Dr Garcia-Bellido, Dr Marc Therrien and Dr D.M. Ruden for kindly providing necessary fly stocks and reagents.

FUNDING

National Institutes of Health (NIH) grants (GM25232 to J.T.L.; CA140730 to J.T.L. and H.H.S.; Minority supplement #25232-2351 to J.T.L. and H.H.S.) and Cornell University (Provost Diversity Fellowship to H.H.S.). Funding for open access charge: NIH.

Conflict of interest statement. None declared.

REFERENCES

1. Biggs,W.H. 3rd, Zavitz,K.H., Dickson,B., van der Straten,A., Brunner,D., Hafen,E. and Zipursky,S.L. (1994) The drosophila rolled locus encodes a MAP kinase required in the sevenless signal transduction pathway. *EMBO J.*, **13**, 1628–1635.
2. Xiao,X., Zuo,X., Davis,A.A., McMillan,D.R., Curry,B.B., Richardson,J.A. and Benjamin,I.J. (1999) HSF1 is required for extra-embryonic development, postnatal growth and protection during inflammatory responses in mice. *EMBO J.*, **18**, 5943–5952.
3. Rabindran,S.K., Giorgi,G., Clos,J. and Wu,C. (1991) Molecular cloning and expression of a human heat shock factor, HSF1. *Proc. Natl Acad. Sci. USA*, **88**, 6906–6910.
4. Sarge,K.D., Zimarino,V., Holm,K., Wu,C. and Morimoto,R.I. (1991) Cloning and characterization of two mouse heat shock factors with distinct inducible and constitutive DNA-binding ability. *Genes Dev.*, **5**, 1902–1911.

5. Schuetz,T.J., Gallo,G.J., Sheldon,L., Tempst,P. and Kingston,R.E. (1991) Isolation of a cDNA for HSF2: Evidence for two heat shock factor genes in humans. *Proc. Natl Acad. Sci. USA*, **88**, 6911–6915.
6. Czarnecka-Verner,E., Yuan,C.X., Scharf,K.D., Englich,G. and Gurley,W.B. (2000) Plants contain a novel multi-member class of heat shock factors without transcriptional activator potential. *Plant Mol. Biol.*, **43**, 459–471.
7. Lindquist,S. and Craig,E.A. (1988) The heat-shock proteins. *Annu. Rev. Genet.*, **22**, 631–677.
8. Wiederrecht,G., Seto,D. and Parker,C.S. (1988) Isolation of the gene encoding the S. cerevisiae heat shock transcription factor. *Cell*, **54**, 841–853.
9. Jedlicka,P., Mortin,M.A. and Wu,C. (1997) Multiple functions of drosophila heat shock transcription factor in vivo. *EMBO J.*, **16**, 2452–2462.
10. Morley,J.F. and Morimoto,R.I. (2004) Regulation of longevity in caenorhabditis elegans by heat shock factor and molecular chaperones. *Mol. Biol. Cell*, **15**, 657–664.
11. Walker,G.A., Thompson,F.J., Brawley,A., Scanlon,T. and Devaney,E. (2003) Heat shock factor functions at the convergence of the stress response and developmental pathways in caenorhabditis elegans. *FASEB J.*, **17**, 1960–1962.
12. Murray,J.I., Whitfield,M.L., Trinklein,N.D., Myers,R.M., Brown,P.O. and Botstein,D. (2004) Diverse and specific gene expression responses to stresses in cultured human cells. *Mol. Biol. Cell*, **15**, 2361–2374.
13. Trinklein,N.D., Murray,J.I., Hartman,S.J., Botstein,D. and Myers,R.M. (2004) The role of heat shock transcription factor 1 in the genome-wide regulation of the mammalian heat shock response. *Mol. Biol. Cell*, **15**, 1254–1261.
14. Dai,C., Whitesell,L., Rogers,A.B. and Lindquist,S. (2007) Heat shock factor 1 is a powerful multifaceted modifier of carcinogenesis. *Cell*, **130**, 1005–1018.
15. Ellington,A.D. and Szostak,J.W. (1990) In vitro selection of RNA molecules that bind specific ligands. *Nature*, **346**, 818–822.
16. Tuerk,C. and Gold,L. (1990) Systematic evolution of ligands by exponential enrichment: RNA ligands to bacteriophage T4 DNA polymerase. *Science*, **249**, 505–510.
17. Sazani,P.L., Larralde,R. and Szostak,J.W. (2004) A small aptamer with strong and specific recognition of the triphosphate of ATP. *J. Am. Chem. Soc.*, **126**, 8370–8371.
18. Shi,H., Fan,X., Sevilimedu,A. and Lis,J.T. (2007) RNA aptamers directed to discrete functional sites on a single protein structural domain. *Proc. Natl Acad. Sci. USA*, **104**, 3742–3746.
19. Bock,L.C., Griffin,L.C., Latham,J.A., Vermaas,E.H. and Toole,J.J. (1992) Selection of single-stranded DNA molecules that bind and inhibit human thrombin. *Nature*, **355**, 564–566.
20. Lee,J.H., Canny,M.D., De Erkenez,A., Krilleke,D., Ng,Y.S., Shima,D.T., Pardi,A. and Jucker,F. (2005) A therapeutic aptamer inhibits angiogenesis by specifically targeting the heparin binding domain of VEGF165. *Proc. Natl Acad. Sci. USA*, **102**, 18902–18907.
21. Fan,X., Shi,H. and Lis,J.T. (2005) Distinct transcriptional responses of RNA polymerases I, II and III to aptamers that bind TBP. *Nucleic Acids Res.*, **33**, 838–845.
22. Sevilimedu,A., Shi,H. and Lis,J.T. (2008) TFIIB aptamers inhibit transcription by perturbing PIC formation at distinct stages. *Nucleic Acids Res.*, **36**, 3118–3127.
23. Shi,H., Hoffman,B.E. and Lis,J.T. (1999) RNA aptamers as effective protein antagonists in a multicellular organism. *Proc. Natl Acad. Sci. USA*, **96**, 10033–10038.
24. White,R.R., Sullenger,B.A. and Rusconi,C.P. (2000) Developing aptamers into therapeutics. *J. Clin. Invest.*, **106**, 929–934.
25. Zhao,X., Shi,H., Sevilimedu,A., Liachko,N., Nelson,H.C. and Lis,J.T. (2006) An RNA aptamer that interferes with the DNA binding of the HSF transcription activator. *Nucleic Acids Res.*, **34**, 3755–3761.
26. Kang,B.H., Plescia,J., Dohi,T., Rosa,J., Doxsey,S.J. and Altieri,D.C. (2007) Regulation of tumor cell mitochondrial homeostasis by an organelle-specific Hsp90 chaperone network. *Cell*, **131**, 257–270.
27. Soti,C., Nagy,E., Giricz,Z., Vigh,L., Csermely,P. and Ferdinandy,P. (2005) Heat shock proteins as emerging therapeutic targets. *Br. J. Pharmacol.*, **146**, 769–780.
28. Xiao,W., Pacyna-Gengelbach,M., Schluns,K., An,Q., Gao,Y., Cheng,S. and Petersen,I. (2005) Differentially expressed genes associated with human lung cancer. *Oncol. Rep.*, **14**, 229–234.
29. Zaarur,N., Gabai,V.L., Porco,J.A. Jr, Calderwood,S. and Sherman,M.Y. (2006) Targeting heat shock response to sensitize cancer cells to proteasome and Hsp90 inhibitors. *Cancer Res.*, **66**, 1783–1791.
30. Sawai,A., Chandarlapaty,S., Greulich,H., Gonen,M., Ye,Q., Arteaga,C.L., Sellers,W., Rosen,N. and Solit,D.B. (2008) Inhibition of Hsp90 down-regulates mutant epidermal growth factor receptor (EGFR) expression and sensitizes EGFR mutant tumors to paclitaxel. *Cancer Res.*, **68**, 589–596.
31. Schwartz,B.E., Werner,J.K. and Lis,J.T. (2004) Indirect immunofluorescent labeling of drosophila polytene chromosomes: visualizing protein interactions with chromatin in vivo. *Methods Enzymol.*, **376**, 393–404.
32. Westwood,J.T., Clos,J. and Wu,C. (1991) Stress-induced oligomerization and chromosomal relocalization of heat-shock factor. *Nature*, **353**, 822–827.
33. Yao,J., Munson,K.M., Webb,W.W. and Lis,J.T. (2006) Dynamics of heat shock factor association with native gene loci in living cells. *Nature*, **442**, 1050–1053.
34. Xiao,H. and Lis,J.T. (1989) Heat shock and developmental regulation of the drosophila melanogaster hsp83 gene. *Mol. Cell. Biol.*, **9**, 1746–1753.
35. Rutherford,S.L. and Lindquist,S. (1998) Hsp90 as a capacitor for morphological evolution. *Nature*, **396**, 336–342.
36. Sollars,V., Lu,X., Xiao,L., Wang,X., Garfinkel,M.D. and Ruden,D.M. (2003) Evidence for an epigenetic mechanism by which Hsp90 acts as a capacitor for morphological evolution. *Nat. Genet.*, **33**, 70–74.
37. Xiao,H., Perisic,O. and Lis,J.T. (1991) Cooperative binding of drosophila heat shock factor to arrays of a conserved 5 bp unit. *Cell*, **64**, 585–593.
38. Saunders,A., Core,L.J. and Lis,J.T. (2006) Breaking barriers to transcription elongation. *Nat. Rev. Mol. Cell Biol.*, **7**, 557–567.
39. Petesch,S.J. and Lis,J.T. (2008) Rapid, transcription-independent loss of nucleosomes over a large chromatin domain at Hsp70 loci. *Cell*, **134**, 74–84.
40. Hanahan,D. and Weinberg,R.A. (2000) The hallmarks of cancer. *Cell*, **100**, 57–70.
41. van der Straten,A., Rommel,C., Dickson,B. and Hafen,E. (1997) The heat shock protein 83 (Hsp83) is required for raf-mediated signalling in drosophila. *EMBO J.*, **16**, 1961–1969.
42. Li,J. and Li,W.X. (2003) Drosophila gain-of-function mutant RTK torso triggers ectopic dpp and STAT signaling. *Genetics*, **164**, 247–258.
43. Nakai,A. and Ishikawa,T. (2001) Cell cycle transition under stress conditions controlled by vertebrate heat shock factors. *EMBO J.*, **20**, 2885–2895.
44. Wang,S., Zhao,X., Suran,R., Vogt,V.M., Lis,J.T. and Shi,H. (2010) Knocking down gene function with an RNA aptamer expressed as part of an intron. *Nucleic Acids Res.*, **38**, e154.
45. Lindquist,S. (1980) Varying patterns of protein synthesis in drosophila during heat shock: Implications for regulation. *Dev. Biol.*, **77**, 463–479.
46. Brugge,J.S., Erikson,E. and Erikson,R.L. (1981) The specific interaction of the rous sarcoma virus transforming protein, pp60src, with two cellular proteins. *Cell*, **25**, 363–372.
47. Oppermann,H., Levinson,A.D., Levintow,L., Varmus,H.E., Bishop,J.M. and Kawai,S. (1981) Two cellular proteins that immunoprecipitate with the transforming protein of rous sarcoma virus. *Virology*, **113**, 736–751.
48. Castrillon,D.H., Gonczy,P., Alexander,S., Rawson,R., Eberhart,C.G., Viswanathan,S., DiNardo,S. and Wasserman,S.A. (1993) Toward a molecular genetic analysis of spermatogenesis in drosophila melanogaster: characterization of male-sterile mutants generated by single P element mutagenesis. *Genetics*, **135**, 489–505.
49. Chakraborty,A., Koldobskiy,M.A., Sixt,K.M., Juluri,K.R., Mustafa,A.K., Snowman,A.M., van Rossum,D.B., Patterson,R.L.

and Snyder,S.H. (2008) HSP90 regulates cell survival via inositol hexakisphosphate kinase-2. *Proc. Natl Acad. Sci. USA*, **105**, 1134–1139.
50. Chen,C.Y. and Balch,W.E. (2006) The Hsp90 chaperone complex regulates GDI-dependent rab recycling. *Mol. Biol. Cell*, **17**, 3494–3507.
51. Lange,B.M., Bachi,A., Wilm,M. and Gonzalez,C. (2000) Hsp90 is a core centrosomal component and is required at different stages of the centrosome cycle in drosophila and vertebrates. *EMBO J.*, **19**, 1252–1262.
52. Yue,L., Karr,T.L., Nathan,D.F., Swift,H., Srinivasan,S. and Lindquist,S. (1999) Genetic analysis of viable Hsp90 alleles reveals a critical role in drosophila spermatogenesis. *Genetics*, **151**, 1065–1079.
53. Pirkkala,L., Nykanen,P. and Sistonen,L. (2001) Roles of the heat shock transcription factors in regulation of the heat shock response and beyond. *FASEB J.*, **15**, 1118–1131.